

The kinks, the solitons and the shocks in series connected discrete Josephson transmission lines

Eugene Kogan^{1,*}

¹*Department of Physics, Bar-Ilan University, Ramat-Gan 52900, Israel*

(Dated: March 30, 2022)

We analytically study wave propagation in the discrete Josephson transmission lines (JTL), constructed from Josephson junctions (JJ) and capacitors. Our approach is based on the quasi-continuum approximation, which we discuss in details. The approximation allows to take into account the intrinsic dispersion in the discrete JTL. Due to competition between such dispersion and the nonlinearity, in the dissipationless JTL there exist running waves in the form of supersonic kinks and solitons. We also study the effect of dissipation in the system and find that in the presence of the resistors, shunting the JJ and/or in series with the ground capacitors, the only possible stationary running waves are the shock waves

PACS numbers:

I. INTRODUCTION

The concept that in a nonlinear wave propagation system the various parts of the wave travel with different velocities, and that wave fronts (or tails) can sharpen into shock waves, is deeply imbedded in the classical theory of fluid dynamics¹. The methods developed in that field can be profitably used to study signal propagation in nonlinear transmission lines²⁻¹¹. In the early studies of shock waves in transmission lines, the origin of the nonlinearity was due to nonlinear capacitance in the circuit¹²⁻¹⁴.

Interesting and potentially important examples of nonlinear transmission lines are circuits containing Josephson junctions (JJ)¹⁵ - Josephson transmission lines (JTL)¹⁶⁻¹⁹. The unique nonlinear properties of JTL allow to construct soliton propagators, microwave oscillators, mixers, detectors, parametric amplifiers, and analog amplifiers¹⁷⁻¹⁹.

Transmission lines formed by JJ connected in series were studied beginning from 1990s, though much less than transmission lines formed by JJ connected in parallel²⁰. However, the former began to attract quite a lot of attention recently²¹⁻²⁸, especially in connection with possible JTL traveling wave parametric amplification²⁹⁻³¹.

The interest in studies of discrete nonlinear electrical transmission lines, in particular of lossy nonlinear transmission lines, has started some time ago³², but it became even more pronounced recently^{33,34}. These studies should be seen in the general context of waves in strongly nonlinear discrete systems³⁵⁻⁴¹.

In our previous publication⁴² we considered shock waves in the continuous JTL with resistors, studying the influence of those on the shock profile. Now we want to analyse wave propagation in the discrete JTL, both lossless and lossy.

The rest of the paper is constructed as follows. In Section II we formulate quasi-continuum approximation for the discrete lossless JTL. In Section III we show that the problem of a running wave is reduced to an effec-

tive mechanical problem, describing motion of a fictitious particle. In Section IV the velocity and the profile of the kink, and in Section V - of the soliton are found from the solution of the effective mechanical problem. In Section VI we rigorously justify the quasi-continuum approximation for the kinks and solitons in certain limiting cases. In Section VII we discuss the effect of dissipation on the waves propagation in the discrete JTL. In Section VIII, we additionally comment on the role of dissipation in the system, and discuss the relation between the quasi-continuum approximation used in the paper, and the quasi-continuous approximation developed some time earlier. We also briefly mention possible applications of the results obtained in the paper and opportunities for their generalization. We conclude in Section IX. In the Appendix A we check up the quasi-continuum approximation by applying it to the linear discrete transmission line. In the Appendix B we propose the integral approximation to the discrete equations.

II. THE QUASI-CONTINUUM APPROXIMATION

Consider the model of JTL constructed from identical JJ and capacitors, which is shown on Fig. 1. We take as dynamical variables the phase differences (which we for brevity will call just phases) φ_n across the JJ and the charges q_n which have passed through the JJ. The circuit equations are

$$\frac{\hbar}{2e} \frac{d\varphi_n}{dt} = \frac{1}{C} (q_{n+1} - 2q_n + q_{n-1}), \quad (1a)$$

$$\frac{dq_n}{dt} = I_c \sin \varphi_n, \quad (1b)$$

where C is the capacitor, and I_c is the critical current of the JJ.

Differentiating Eq. (1a) with respect to t and substituting dq_n/dt from Eq. (1b), we obtain closed equation

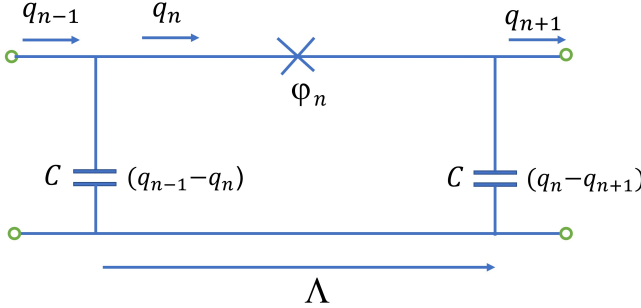


FIG. 1: Discrete JTL.

for φ_n ⁴²⁻⁴⁵

$$\frac{d^2\varphi_n}{d\tau^2} = \sin \varphi_{n+1} - 2 \sin \varphi_n + \sin \varphi_{n-1}, \quad (2)$$

where $L_J = \hbar/(2eI_c)$, and we have introduced the dimensionless time $\tau = t/\sqrt{L_J C}$. It is interesting to compare Eq. (2) with a discrete sine-Gordon equation for lattice wave field³⁹

$$\frac{d^2\varphi_n}{d\tau^2} - D(\varphi_{n+1} - 2\varphi_n + \varphi_{n-1}) + \sin \varphi = 0,$$

where D is some constant, and a sine-lattice discrete double sine-Gordon equation⁴⁶

$$\begin{aligned} \frac{d^2u_n}{d\tau^2} - \sin(u_{n+1} - u_n) + \sin(u_n - u_{n-1}) \\ = g(-\sin u_{n-1} + \eta \sin 2u_n), \end{aligned}$$

where g and η are some constants.

Everywhere in this paper we'll treat $\varphi_n(t)$ ($q_n(t)$) as a function of two continuous variables (z, t) , where $z = n\Lambda$. Hence we can write down Eq. (2) symbolically as

$$\frac{\partial^2\varphi}{\partial z^2} = 2 \sum_{m=1}^{\infty} \frac{\Lambda^{2m}}{(2m)!} \frac{\partial^{2m} \sin \varphi}{\partial z^{2m}}, \quad (3)$$

where Λ is the period of the line. The question how many terms can and should be kept in the sum in the r.h.s. of Eq. (3) is far from being trivial. If we keep only a single term, we obtain the continuum approximation, which attracts by its simplicity. However the phenomena we'll be talking about are absent in this approximation. So we make the next simplest assumption, by truncating the sum after the first two terms. In the previous Section we approximated the wave only far from the kink, now, to find the profile of the kink, we need to do it everywhere. After the truncation we obtain a solvable equation for $\varphi(z, \tau)$ in the form

$$\frac{1}{\Lambda^2} \frac{\partial^2\varphi}{\partial z^2} = \frac{\partial^2 \sin \varphi}{\partial z^2} + \frac{\Lambda^2}{12} \frac{\partial^4 \sin \varphi}{\partial z^4}, \quad (4)$$

thus reducing the original system of ordinary differential equations (1) to a single partial differential equation. We will call such truncation the quasi-continuum approximation. We'll see later that in certain limiting cases we can rigorously justify the quasi-continuum approximation.

III. NEWTONIAN EQUATION

The running wave solutions are of the form

$$\varphi(z, t) = \varphi(x), \quad q(z, t) = q(x), \quad (5)$$

where $x = \bar{U}t - z$, and U is the running wave velocity. (in this paper, for any velocity V , $\bar{V} \equiv V\sqrt{L_J C}/\Lambda$).

For such solutions we obtain an ordinary differential equation

$$\frac{\Lambda^2}{12} \frac{d^4 \sin \varphi}{dx^4} + \frac{d^2 \sin \varphi}{dx^2} - \bar{U}^2 \frac{d^2 \varphi}{dx^2} = 0. \quad (6)$$

Integrating with respect to x twice, we obtain

$$\frac{\Lambda^2}{12} \frac{d^2 \sin \varphi}{dx^2} = -\sin \varphi + \bar{U}^2 \varphi + F, \quad (7)$$

where F is the constant of integration. The other constant of integration is equal to zero because of the boundary conditions. Equation (7) can be considered as the balance between the dispersion effects, described by the l.h.s. of the equation, and the nonlinear effects described by the (nonlinear terms of the) r.h.s. of the equation.

Multiplying Eq. (7) by $d \sin \varphi / dx$ and integrating once again we obtain

$$\frac{\Lambda^2}{24} \left(\frac{d \sin \varphi}{dx} \right)^2 + \Pi(\sin \varphi) = E, \quad (8)$$

where

$$\Pi(\sin \varphi) = \frac{1}{2} \sin^2 \varphi - \bar{U}^2 (\varphi \sin \varphi + \cos \varphi) - F \sin \varphi, \quad (9)$$

and E is another constant of integration. Equation (8) can be integrated in quadratures in the general case.

We can think about x as time and about $\sin \varphi$ as coordinate of the fictitious particle, thus considering (7) as the Newtonian equation. We are interested in the propagation of the waves characterised by the boundary conditions

$$\lim_{x \rightarrow -\infty} \varphi = \varphi_1, \quad \lim_{x \rightarrow +\infty} \varphi = \varphi_2, \quad (10)$$

(this explains presence of only one integration constant in Eq. (7)). The problem of finding the profile of the wave is reduced to studying the motion of the particle which, because of the boundary conditions starts from an equilibrium position, and ends in an equilibrium position.

Using the expertise we acquired in mechanics classes, we come to the conclusion that the initial position corresponds to maxima of the "potential energy" $\Pi(\sin \varphi)$, and so does the final position. Either these are two different maxima, or the same maximum. In the latter case the particle returns to the initial position after reflection from a potential wall. (See Figs. 2 (above) and 3.) In the first case the solution describes the kink, in the second - the soliton.

From the fact that there is a maximum of the "potential energy" at the point φ_1 , follows that

$$\frac{d^2\Pi(\varphi)}{d\varphi^2}\bigg|_{\varphi=\varphi_1} < 0. \quad (11)$$

Calculating the derivatives we obtain

$$\bar{U}^2 > \cos \varphi_1, \quad (12)$$

that is the running wave is supersonic.

IV. THE KINKS

In the case of the kink, going in Eq. (7) to the limits $x \rightarrow +\infty$ and $x \rightarrow -\infty$ we obtain

$$\bar{U}^2 \varphi_1 = \sin \varphi_1 - F, \quad (13a)$$

$$\bar{U}^2 \varphi_2 = \sin \varphi_2 - F. \quad (13b)$$

Solving (13) relative to \bar{U}^2 and F we obtain we obtain

$$\bar{U}^2 = \frac{\sin \varphi_1 - \sin \varphi_2}{\varphi_1 - \varphi_2} \equiv \bar{U}_{\text{sh}}^2(\varphi_1, \varphi_2), \quad (14a)$$

$$F = \frac{\varphi_1 \sin \varphi_2 - \varphi_2 \sin \varphi_1}{\varphi_1 - \varphi_2}; \quad (14b)$$

the reason, why we have chosen subscript sh for the velocity in (14a), will become clear in Section VII. Taking into account the equality

$$E = \Pi(\sin \varphi_1) = \Pi(\sin \varphi_2), \quad (15)$$

we obtain

$$\varphi_2 = -\varphi_1. \quad (16)$$

Thus the kinks which can propagate in JTL are very special. We also obtain

$$F = 0, \quad (17a)$$

$$\bar{U}^2 = \bar{U}_{\text{sh}}^2(\varphi_1, -\varphi_1) = \frac{\sin \varphi_1}{\varphi_1} \equiv \bar{U}_k^2(\varphi_1). \quad (17b)$$

$$\begin{aligned} \Pi(\sin \varphi) - E &= \frac{1}{2}(\sin \varphi - \sin \varphi_1)^2 \\ &- \frac{\sin \varphi_1}{\varphi_1} [\cos \varphi - \cos \varphi_1 - (\varphi_1 - \varphi) \sin \varphi]. \end{aligned} \quad (17c)$$

One should compare the kink velocity with the velocity $u(\varphi_1)$ of propagation along the JTL of small amplitude smooth disturbances of φ on a homogeneous background φ_1 ⁴²

$$\bar{u}^2(\varphi_1) = \cos \varphi_1 \quad (18)$$

(in this paper we consider only the solutions which lie completely in the sector $(-\pi/2, \pi/2)$.)

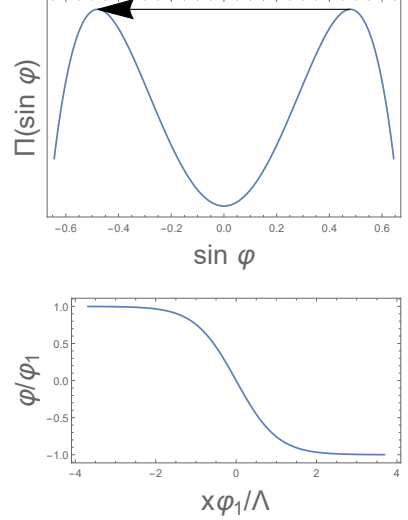


FIG. 2: The "potential energy" (17c) (above) and the kink profile calculated with this energy according to Eq. (8) (below). We have chosen $\varphi_1 = .5$.

Equation (17c) and the results of integration of Eq. (8) for this "potential energy" are graphically presented on Fig. 2 (above).

Consider specifically the limiting case $|\varphi_1| \ll 1$. Expanding the "potential energy" with respect to φ and φ_1 and keeping only the lowest order terms we obtain the approximation to Eq. (8) in the form

$$\Lambda^2 \left(\frac{d\varphi}{dx} \right)^2 = (\varphi_1^2 - \varphi^2)^2. \quad (19)$$

The solution of Eq. (19) is

$$\varphi(x) = -\varphi_1 \tanh \frac{\varphi_1 x}{\Lambda}. \quad (20)$$

Equations (20) coincides with that obtained by Katayama et al.⁴⁵. So does Eq. (17b), being expanded in series with respect to φ_1 and truncated after the first two terms:

$$\bar{U}_k(\varphi_1) = 1 - \frac{\varphi_1^2}{12}. \quad (21)$$

V. THE SOLITONS

For the soliton $\varphi_2 = \varphi_1$, and two equations of (13) become one equation. As an additional parameter we take the amplitude of the soliton (maximally different from φ_1 value of φ), which we will designate as φ_0 . Adding to (13) the equation

$$E = \Pi(\sin \varphi_0) = \Pi(\sin \varphi_1) \quad (22)$$

and solving the obtained system we obtain

$$\bar{U}_{sol}^2(\varphi_1, \varphi_0) = \frac{(\sin \varphi_1 - \sin \varphi_0)^2}{2[\cos \varphi_0 - \cos \varphi_1 - (\varphi_1 - \varphi_0) \sin \varphi_0]}, \quad (23a)$$

$$\Pi(\sin \varphi) - E = \frac{1}{2} (\sin \varphi_1 - \sin \varphi)^2 - \bar{U}_{sol}^2(\varphi_1, \varphi_0) \cdot [\cos \varphi - \cos \varphi_1 - (\varphi_1 - \varphi) \sin \varphi]. \quad (23b)$$

Equation (23b) is graphically presented on Fig. 3.

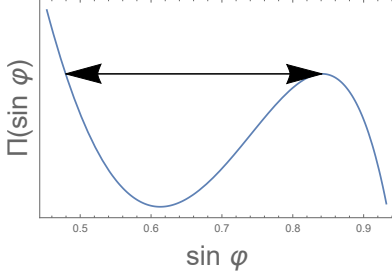


FIG. 3: The "potential energy" (23b). We have chosen $\varphi_1 = 1.0$ and $\varphi_0 = .5$.

Considering the limiting case $|\varphi_1|, |\varphi_0| \ll 1$, expanding Eq. (23b) with respect to all the phases and keeping only the lowest order terms we obtain Eq. (8) in the form

$$\Lambda^2 \left(\frac{d\varphi}{dx} \right)^2 = (\varphi - \varphi_1)^2 (\varphi - \varphi_0) (\varphi + 2\varphi_1 + \varphi_0). \quad (24)$$

Equation (24) can be integrated in elementary functions

$$\varphi = \varphi_1 - \frac{(4\bar{\varphi} + \Delta\varphi)\Delta\varphi}{4\bar{\varphi} \cosh^2 \Phi + \Delta\varphi}, \quad (25)$$

where

$$\Delta\varphi \equiv \varphi_1 - \varphi_0, \quad (26a)$$

$$\bar{\varphi} \equiv (\varphi_1 + \varphi_0)/2, \quad (26b)$$

$$\Phi \equiv \sqrt{(3\varphi_1 + \varphi_0)\Delta\varphi} x/(2\Lambda). \quad (26c)$$

Equation (25) is graphically presented on Fig. 4. The result looks like a dark soliton, but if we were plotting the supercurrent instead of the phase, which arguably would have been more meaningful, it would look like a bright soliton.

In an another limiting case of weak soliton ($\Delta\varphi \cot \varphi_1 \ll 1$), Eq. (8) takes the form

$$\Lambda^2 \left(\frac{d\varphi}{dx} \right)^2 = 4 \tan \varphi_1 \cdot (\varphi - \varphi_1)^2 (\varphi - \varphi_0). \quad (27)$$

The solution of Eq. (27) is

$$\varphi = \varphi_1 - \Delta\varphi \operatorname{sech}^2 \left(\sqrt{\Delta\varphi \tan \varphi_1} x/\Lambda \right). \quad (28)$$

Velocity of the soliton in this approximation is

$$\bar{U}_{sol}(\varphi_1, \varphi_0) = \sqrt{\cos \varphi_1} \left(1 - \frac{1}{6} \tan \varphi_1 \Delta\varphi \right). \quad (29)$$

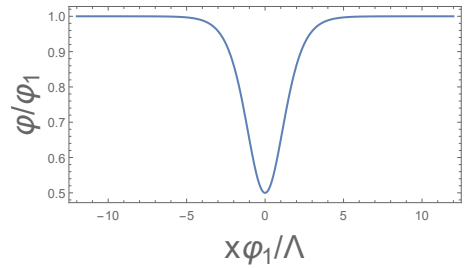


FIG. 4: The soliton profile according to Eq. (25). We have chosen $\varphi_0 = .5\varphi_1$.

VI. THE CONTROLLED QUASI-CONTINUUM APPROXIMATION

Let us return to Eq. (2). Looking at Eqs. (20) and (25) we realize that in the description of the kinks and solitons with $|\varphi_1| \ll 1$, the expansion parameter in the r.h.s. of Eq. (3) is φ_1^2 ; thus the quasi-continuum approximation (4) can be rigorously justified. However, strictly speaking, truncation of the expansion should be performed in accordance with the truncation of the series expansion of the sine function, and Eq. (4), in the consistent approximation should be written as

$$\frac{1}{\Lambda^2} \frac{\partial^2 \varphi}{\partial \tau^2} = \frac{\partial^2 \varphi}{\partial z^2} - \frac{1}{6} \frac{\partial^2 \varphi^3}{\partial z^2} + \frac{\Lambda^2}{12} \frac{\partial^4 \varphi}{\partial z^4}. \quad (30)$$

Equation (30) clearly shows the competition between the nonlinearity, described by the second term in the r.h.s. of the equation, and the intrinsic dispersion, caused by the discreteness of the line, described by the third term. Same as true for Eq. (32) below. If we put in Eq. (20)

$$x = \Lambda \left(1 - \frac{\varphi_1^2}{12} \right) \tau - z, \quad (31)$$

the obtained result would be an exact solution of Eq. (30). Note that (30) is applicable not only to the kinks. Any small phase ($\varphi \ll 1$) waves can be described by this equation.

Looking at Eq. (28) we realize alternatively, that the quasi-continuum approximation can be rigorously justified when it is applied to the description of the solitons with $\tan \varphi_1 \cdot (\varphi_1 - \varphi_0) \ll 1$. The latter quantity is the expansion parameter in the r.h.s. of Eq. (3) in this case. So in the consistent approximation, Eq. (4) should be written as

$$\frac{1}{\Lambda^2} \frac{\partial^2 \psi}{\partial \tau^2} = \cos \varphi_1 \frac{\partial^2 \psi}{\partial z^2} - \frac{\sin \varphi_1}{2} \frac{\partial^2 \psi^2}{\partial z^2} + \cos \varphi_1 \frac{\Lambda^2}{12} \frac{\partial^4 \psi}{\partial z^4}, \quad (32)$$

where $\psi = \varphi - \varphi_1$. Looking at Eq. (32) we recognize Boussinesq equation. If we put in Eq. (28)

$$x = \Lambda \sqrt{\cos \varphi_1} \left(1 - \frac{\tan \varphi_1}{6} \Delta\varphi \right) \tau - z, \quad (33)$$

the obtained result would be an exact solution of Eq. (32). Note also that (32) is applicable not only to the solitons. Any weak (in the sense that the phase doesn't deviate much from the constant background value φ_1) wave can be described by this equation. Some indications to how good is the quasi-continuum approximation outside the regions when it is controlled see in the Appendix A.

Here we would like to attract the attention of the reader to the following issue. Common wisdom says that the continuum approximation and the small amplitude approximation are independent - there could be a wave with small amplitude, which allows to expand the sine function, but which varies fast in space (wavelength comparable to lattice spacing), so the continuum limit is not justified. And there could be the opposite situation (large amplitude, long wavelength), in which the sine needs to be retained but the continuum limit is allowed.

However, for the kinks and the solitons these approximations are not independent. Parametrically, the length scale of the waves is of the order of the lattice spacing Λ , so, naively, the continuum (or even the quasi-continuum) limit is not justified. What we have shown above, is that for the waves with small amplitude $|\varphi_1|$ ($\tan \varphi_1 (\varphi_1 - \varphi_0)$), the length scale is $\Lambda/|\varphi_1|$ ($\Lambda/(\tan \varphi_1 (\varphi_1 - \varphi_0))$), thus justifying the quasi-continuum approximation.

A. The simple wave approximation

Consider the controlled quasi-continuum approximation. Let us, on top of it, make a simple wave approximation. We start from writing down Eq. (4) as

$$\frac{1}{\Lambda^2} \frac{\partial^2 \varphi}{\partial \tau^2} = \left[\left(\frac{\partial^2}{\partial z^2} + \frac{\Lambda^2}{12} \frac{\partial^4}{\partial z^4} \right) \left(1 - \frac{1}{6} \hat{O}^2 + \frac{1}{120} \hat{O}^4 + \dots \right) \right] \varphi, \quad (34)$$

where \hat{O} is an operator defined by the relation $\hat{O}\phi = \phi$ for any phase ϕ , that is the operator by itself doesn't bear any traces of φ . The simple wave approximation is obtained by changing by brute force the wave equation into two decoupled equations for right and left going waves¹⁴ (see also the Appendix A). We can reach the aim by taking (approximately) the square root from the operators standing both in the l.h.s., and in the r.h.s. of the equation, and writing down

$$\frac{1}{\Lambda} \frac{\partial \varphi}{\partial \tau} = \pm \left[\left(\frac{\partial}{\partial z} + \frac{\Lambda}{24} \frac{\partial^3}{\partial z^3} \right) \left(1 - \frac{1}{12} \hat{O}^2 + \dots \right) \right] \varphi. \quad (35)$$

Opening the parenthesis and the brackets, we obtain, leaving only the leading terms,

$$\frac{1}{\Lambda} \frac{\partial \varphi}{\partial \tau} = \pm \left(\frac{\partial \varphi}{\partial z} - \frac{1}{12} \frac{\partial \varphi^3}{\partial z} + \frac{\Lambda^2}{24} \frac{\partial^3 \varphi}{\partial z^3} \right), \quad (36)$$

which is modified Korteweg-de Vries (mKdV) equation⁴⁵. If we put in Eq. (20)

$$x = \Lambda \left(1 - \frac{\varphi_1^2}{12} \right) \tau - z, \quad (37)$$

the obtained result would be an exact solution of Eq. (36).

Let us make the same trick for weak waves, that is let us write down $\varphi = \varphi_1 + \psi$, and present Eq. (4) as an expansion with respect to ψ by writing down Eq. (4) as

$$\frac{1}{\Lambda^2} \frac{\partial^2 \psi}{\partial \tau^2} = \left[\left(\frac{\partial^2}{\partial z^2} + \frac{\Lambda^2}{12} \frac{\partial^4}{\partial z^4} \right) \left(\cos \varphi_1 - \frac{\sin \varphi_1}{2} \hat{O} + \dots \right) \right] \psi. \quad (38)$$

Taking the square root from both parts of the equation we get

$$\frac{1}{\Lambda} \frac{\partial \psi}{\partial \tau} = \pm \sqrt{\cos \varphi_1} \left[\left(\frac{\partial}{\partial z} + \frac{\Lambda}{24} \frac{\partial^3}{\partial z^3} \right) \left(1 - \frac{\tan \varphi_1}{4} \hat{O} + \dots \right) \right] \psi. \quad (39)$$

Opening the parenthesis and the brackets, we obtain, leaving only the leading terms,

$$\frac{1}{\Lambda} \frac{\partial \psi}{\partial \tau} = \pm \sqrt{\cos \varphi_1} \left(\frac{\partial \psi}{\partial z} - \frac{\tan \varphi_1}{4} \frac{\partial \psi^2}{\partial z} + \frac{\Lambda^2}{24} \frac{\partial^3 \psi}{\partial z^3} \right), \quad (40)$$

which is KdV equation. If we put in Eq. (28)

$$x = \Lambda \sqrt{\cos \varphi_1} \left(1 - \frac{\tan \varphi_1}{6} \Delta \varphi \right) \tau - z, \quad (41)$$

the obtained result would be an exact solution of Eq. (40).

VII. THE SHOCKS

Consider JTL with the capacitor and resistor shunting the JJ and another resistor in series with the ground capacitor, shown on Fig. 5. As the result, Eq. (1) changes to

$$\frac{\hbar}{2e} \frac{d\varphi_n}{dt} = \left(\frac{1}{C} + R \frac{\partial}{\partial t} \right) (q_{n+1} - 2q_n + q_{n-1}), \quad (42a)$$

$$\frac{dq_n}{dt} = I_c \sin \varphi_n + \frac{\hbar}{2eR_J} \frac{d\varphi_n}{dt} + C_J \frac{\hbar}{2e} \frac{d^2 \varphi_n}{dt^2}, \quad (42b)$$

where R is the ohmic resistor in series with the ground capacitor, and C_J and R_J are the capacitor and the ohmic resistor shunting the JJ. Equation (42b) takes into account that now the current passes through three parallel branches. Equation (4) changes to

$$\frac{L_J C_J}{\Lambda^2} \frac{\partial^2 \varphi}{\partial t^2} = \left(1 + RC \frac{\partial}{\partial t} \right) \left(\frac{\partial^2}{\partial z^2} + \frac{\Lambda^2}{12} \frac{\partial^4}{\partial z^4} \right) \cdot \left(\sin \varphi + \frac{L_J}{R_J} \frac{\partial \varphi}{\partial t} + L_J C_J \frac{\partial^2 \varphi}{\partial t^2} \right). \quad (43)$$

Opening the parenthesis in Eq. (43) and considering the running wave solutions we obtain

$$\frac{\Lambda^2}{12} \frac{d^2 \sin \varphi}{dx^2} + \left(\frac{C_J}{C} + \frac{R}{R_J} \right) \bar{U}^2 \Lambda^2 \frac{d^2 \varphi}{dx^2} + \left(\frac{R}{Z_J} \cos \varphi + \frac{Z_J}{R_J} \right) \bar{U} \Lambda \frac{d\varphi}{dx} = -\sin \varphi + \bar{U}^2 \varphi + F, \quad (44)$$

where $Z_J \equiv \sqrt{L_J/C}$ is the characteristic impedance of the JTL, and we discarded the terms with the derivatives higher than of the forth order.

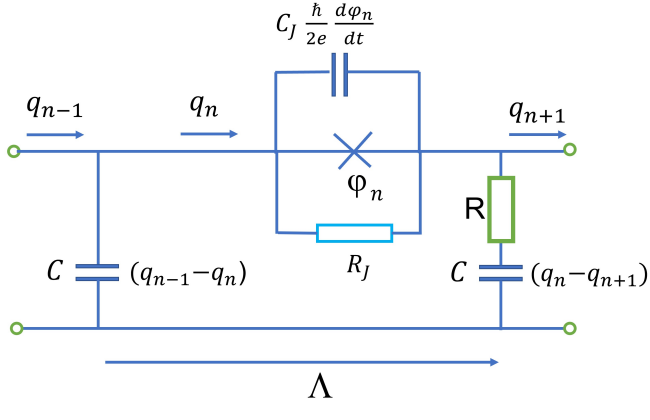


FIG. 5: Discrete JTL with the capacitor and the resistor shunting the JJ and another resistor in series with the ground capacitor

We impose the boundary conditions (10) and try to understand what part of the analysis of Section III can be transferred to the present case. The results (13) are determined only by the r.h.s. of Eq. (7), so are (??), following from (13). Since the r.h.s. of Eqs. (7) and (44) are identical, these equations are valid in the present case also. In particular, we obtain

$$\bar{U}^2 = \bar{U}_{\text{sh}}^2(\varphi_1, \varphi_2), \quad (45)$$

which explains the subscript we introduced in Eq. (14a).

Looking at Eq. (44) we understand, that when C_J and/or R are large enough, and/or R_J is small enough the first term in the l.h.s. of (44) can be discarded, hence the continuum approximation valid, and (44) acquires Newtonian form⁴²

$$\left(\frac{C_J}{C} + \frac{R}{R_J} \right) \frac{d^2 \varphi}{d\tau^2} + \left(\frac{R}{Z_J} \cos \varphi + \frac{Z_J}{R_J} \right) \frac{d\varphi}{d\tau} = -\sin \varphi + \bar{U}^2 \varphi + F. \quad (46)$$

Newtonian form being achieved, we realize that the resistors, by introducing the effective "friction force", break the "energy" conservation law, which means that the stationary kinks and the solitons we considered previously are no longer possible, however weak the dissipation is. In distinction from case of the kinks and the solitons, now

the fictitious particle trajectory connects the "potential energy" maximum with the "potential energy" minimum, which allows in the lossy JTL the shocks with $|\varphi_2| \neq |\varphi_1|$. Actually, what we are saying in this paragraph is valid not only for (46), but for (44) in general.

The shocks in the framework of the continuum approximation were studied in our previous publication⁴². In particular, in the simple case when $C_J = 0$, $R = 0$ (when (46) is similar to equation describing the motion of a fluxon in biased long JJ³⁹) and for weak shock ($\Delta\varphi \cdot \cot \varphi_1 \ll 1$), where $\Delta\varphi \equiv (\varphi_1 - \varphi_2)/2$, Eq. (46) takes the form

$$\frac{Z_J}{R_J} \frac{d\psi}{d\tau} = \sin \bar{\varphi} (\psi^2 - \Delta^2 \varphi), \quad (47)$$

where $\bar{\varphi} \equiv (\varphi_1 + \varphi_0)/2$ and $\psi \equiv \varphi - \bar{\varphi}$. The solution of (47) is

$$\psi = -\Delta\varphi \tanh \left(\frac{R_J}{Z_J} \Delta\varphi \sin \bar{\varphi} \cdot \tau \right). \quad (48)$$

For qualitative analysis of Eq. (44) in the general case, it is better to present it as a system of two first order differential equations

$$\left[\frac{\cos \varphi}{12} + \left(\frac{C_J}{C} + \frac{R}{R_J} \right) \bar{U}^2 \right] \Lambda \frac{d\chi}{dx} = \frac{\sin \varphi}{12} \chi^2 - \left(\frac{R}{Z_J} \cos \varphi + \frac{Z_J}{R_J} \right) \bar{U} \chi - \sin \varphi + \bar{U}^2 \varphi + F, \quad (49a)$$

$$\Lambda \frac{d\varphi}{dx} = \chi. \quad (49b)$$

Now, from the condition that $(\chi, \varphi) = (0, \varphi_1)$ and $(\chi, \varphi) = (0, \varphi_2)$ are the fixed points of (49), we recover (13).

One important feature of shocks can be understood immediately. We are talking about the direction of shock propagation. Linearising Eq. (49) in the vicinity of the fixed points we obtain

$$\Lambda \begin{pmatrix} d\chi/dx \\ d\varphi/dx \end{pmatrix} = \begin{pmatrix} M_i & K_i \\ 1 & 0 \end{pmatrix} \begin{pmatrix} \varphi - \varphi_i \\ \chi \end{pmatrix}, \quad i = 1, 2 \quad (50)$$

where

$$K_i = \frac{\bar{U}^2 - \cos \varphi_i}{\cos \varphi_i/12 + (C_J/C + R/R_J) \bar{U}^2}, \quad (51)$$

and here we are not interested in M_i . From the fact that φ_1 is the unstable fixed point, and φ_2 is the stable fixed point we obtain

$$\cos \varphi_2 > \bar{U}_{\text{sh}}^2(\varphi_1, \varphi_2) > \cos \varphi_1. \quad (52)$$

The inequalities (52) allow only one direction of shock propagation - from larger $\cos \varphi$ to smaller $\cos \varphi$. Taking into account (18), we can present (52) as

$$\bar{u}^2(\varphi_2) > \bar{U}_{\text{sh}}^2(\varphi_1, \varphi_2) > \bar{u}^2(\varphi_1), \quad (53)$$

thus establishing the connection with the well known in the nonlinear waves theory fact: the shock velocity is lower than the sound velocity in the region behind the shock, but higher than the sound velocity in the region before the shock¹.

Let us write down inequalities (52) explicitly

$$\cos \varphi_2 > \frac{\sin \varphi_1 - \sin \varphi_2}{\varphi_1 - \varphi_2} > \cos \varphi_1. \quad (54)$$

We will combine the case we studied up to now, when φ_1 was the phase before the shock and φ_2 - behind the shock, with the opposite case, which corresponds to indices 1 and 2 in (54) being interchanged.

The points in the phase space of the shock boundary conditions (φ_1, φ_2) , for which neither (54), nor its interchanged version are satisfied, has very simple geometric property. The point (φ_1, φ_2) belongs to that region, if the secant of the curve $\sin \varphi$ between the points φ_1 and φ_2 crosses the curve, like it is shown on Fig. 6 (below). Because $\sin \varphi$ is concave downward for $0 < \varphi < \pi/2$, and concave upward for $-\pi/2 < \varphi < 0$, it never happens if φ_1, φ_2 have the same sign. Hence the shock can exist between any such points. It is not so for φ_1 and φ_2 having opposite signs. We present the phase space of shock boundary conditions on Fig. 6 (above). The forbidden region is shaded.

When the asymptotic phases on the two sides of the JTL belong to the shaded region, probably there exists some intermediate φ_{in} in between, such that the shocks between φ_1 and φ_{in} , and between φ_2 and φ_{in} are allowed. Say, when the phases are φ_1 and $-\varphi_1$, the system can chose the intermediate value $\varphi_{in} = 0$. In this hypothetical case, the shocks move in the opposite directions, and the central part with the phase $\varphi_{in} = 0$ expands with the velocity $2U_{sh}(\varphi_1, 0)$. However, the case of multiple shocks being simultaneously present in the system demands further studies.

Equation (44) can be easily integrated numerically. For aesthetical reasons let us simplify it by putting $R = 0$ and $C_J = 0$. (Actually, the physical meaning and the relevance of the resistor in series with the ground capacitor is not obvious. We included it because we were able to do it for free. The capacitance of the JJ is certainly physically relevant. Anyhow, when $C_J/C \ll 1$, it can be ignored.) After the simplification and substitution of the results for \bar{U} and F from (??), the equation becomes

$$\frac{\cos \varphi}{12} \Lambda^2 \frac{d^2 \varphi}{dx^2} = \frac{\sin \varphi}{12} \left(\frac{d\varphi}{dx} \right)^2 - \frac{Z_J \bar{U} \Lambda}{R_J} \frac{d\varphi}{dx} - \frac{(\sin \varphi - \varphi_2)(\varphi_1 - \varphi) - (\sin \varphi_1 - \sin \varphi)(\varphi - \varphi_2)}{\varphi_1 - \varphi_2}. \quad (55)$$

The result of the numerical integration are shown on Fig. 7 (compare with Figs. 2 (below) and 4).

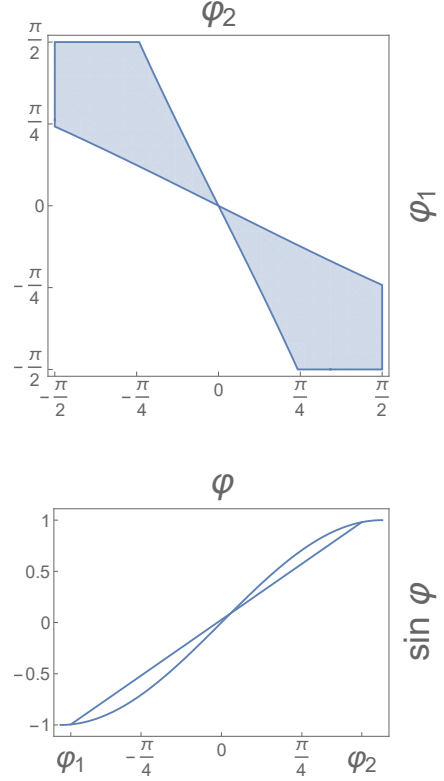


FIG. 6: The phase space of the boundary conditions on the ends of the JTL φ_1 and φ_2 . The region, which corresponds to the forbidden shock boundary conditions, is shaded (above). The geometric property of the points belonging to the shaded region (below).

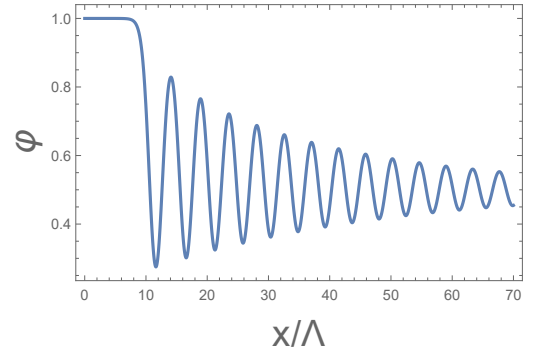


FIG. 7: The shock profile according to Eq. (55). We have chosen $\varphi_1 = 1$, $\varphi_2 = .5$, $Z_J/R_J = .005$.

VIII. DISCUSSION

We would like to additionally discuss the role of dissipation in discrete systems. Dissipation is always present in real experiments. And yet we can observe solitary waves (though they are nonstationary, but practically identical to the corresponding stationary solitons at any given moment of time) in case if dissipation is weak enough. Thus, weak dissipation does not com-

pletely kill solitary waves, it just makes them nonstationary/attenuating. Such solitary waves are observed in numerical calculations and in experiments, as was the case with granular chains^{38,40}. It turns out that there is a critical rate of dissipation which transforms oscillating stationary shock waves into monotonous, both are stationary⁴⁷.

The second issue which needs to be discussed is the relation between the quasi-continuum approximation we use and the quasi-continuous approximation developed some time earlier³². We would like here how the equations of the main body of the paper would have changed if we have used the latter instead of the former.

We reproduce here our Eq. (4)

$$\frac{1}{\Lambda^2} \frac{\partial^2 \varphi}{\partial \tau^2} = \frac{\partial^2 \sin \varphi}{\partial z^2} + \frac{\Lambda^2}{12} \frac{\partial^4 \sin \varphi}{\partial z^4}. \quad (56)$$

In the quasi-continuous approximation we would have got

$$\frac{1}{\Lambda^2} \frac{\partial^2 \varphi}{\partial \tau^2} = \frac{\partial^2 \sin \varphi}{\partial z^2} + \frac{\Lambda^2}{12} \frac{\partial^4 \sin \varphi}{\partial z^2 \partial \tau^2}. \quad (57)$$

Our Eq. (7)

$$\frac{\Lambda^2}{12} \frac{d^2 \sin \varphi}{dx^2} = -\sin \varphi + \bar{U}^2 \varphi + F, \quad (58)$$

would have become

$$\bar{U}^2 \frac{\Lambda^2}{12} \frac{d^2 \sin \varphi}{dx^2} = -\sin \varphi + \bar{U}^2 \varphi + F. \quad (59)$$

It is explained in Section VII that the velocity of the running wave is determined by the r.h.s. of the equations, so the results for the velocities of kinks, solitons and shock would have been identical to ours. We emphasise this fact by stating the Eqs. (7) and (59) are identical, apart from the renormalization of the "microscopic" parameter Λ , but the velocities do not contain this parameter. Similar, the profiles we have obtained would have remained the same, save the scale changed by the factor of \bar{U} , which, in any case, is close to one in most situations.

An advantage of the quasi-continuous approximation is that it is regular at short wavelengths, while ours provides a phenomenological description valid for not too short wavelengths. Apart from that, we can not say which approximation is more true to life. As an advantage of the quasi-continuum approximation we would mention the easy way to the simple wave approximation and an opportunity for a step forward, which we present in the Appendix B and are planning to follow in future.

Recently, quantum mechanical description of JTL in general and parametric amplification in such lines in particular started to be developed, based on quantisation techniques in terms of discrete mode operators⁴⁸, continuous mode operators⁴⁹, a Hamiltonian approach in the Heisenberg and interaction pictures⁵⁰, the quantum Langevin method⁵¹, or on partitions a quantum device into compact lumped or quasi-distributed cells⁵². It

would be interesting to understand in what way the results of the present paper are changed by quantum mechanics. Particularly interesting looks studying of quantum ripples over a semi-classical shock⁵³ and fate of quantum shock waves at late times⁵⁴. Closely connected problem of classical and quantum dispersion-free coherent propagation in waveguides and optical fibers was studied recently in Ref.⁵⁵.

Finally, we would like to express our hope that the results obtained in the paper are applicable to kinetic inductance based traveling wave parametric amplifiers based on a coplanar waveguide architecture. Onset of shock-waves in such amplifiers is an undesirable phenomenon. Therefore, shock waves in various JTL should be further studied, which was one of motivations of the present work.

IX. CONCLUSIONS

We analyzed the quasi-continuum approximation for the discrete JTL. The approximation becomes controllable for the case of Josephson phase difference across the JJ being small and for the case of small amplitude disturbances of the phases on a homogeneous background. The approximation is applied to study the kinks and the solitons which can propagate along the line. The width of such waves turns out to be of the order of the line period. We also study the effect of losses in the system and find that in the presence of the resistors, shunting the JJ and/or in series with the ground capacitors, the only possible stationary running waves are the shock waves. We have proposed the integral approximation, which is alternative to the quasi-continuum approximation.

Acknowledgments

The main idea of the present work was born in the discussions with M. Goldstein. We are also grateful to J. Cuevas-Maraver, A. Dikande, M. Inc, P. Kevrekidis, B. A. Malomed, V. Nesterenko, and B. Ya. Shapiro for their comments (some of which were crucial for the completion of the project) and to P. Rosenau for his criticism. T. H. A. van der Reep read the manuscript and suggested numerous textual corrections which were accepted with gratitude.

Appendix A: Propagator for the discrete linear transmission line

In the Appendix we consider the discrete linear transmission line, obtained from that presented on Fig. 1, by substituting linear inductor for the JJ. The circuit equations are

$$L \frac{d^2 q_n}{dt^2} = \frac{1}{C} (q_{n+1} - 2q_n + q_{n-1}), \quad (A1)$$

where C is the capacitor, and L is the inductance. Introducing the dimensionless time $\tau = t/\sqrt{LC}$ we obtain

$$\frac{d^2 q_n(\tau)}{d\tau^2} = q_{n+1}(\tau) - 2q_n(\tau) + q_{n-1}(\tau). \quad (\text{A2})$$

Because the system is linear (but dispersive), it does not allow solitons, and thus seems to lie outside the scope of the paper. However, we will use the system to check up the (analogue of) Eq. (4) by comparing the exact and the approximate solutions for the propagator.

1. The exact solution

We define the propagator by the initial and the boundary conditions

$$q_n(0) = \delta_{n0}, \quad \dot{q}_n(0) = 0, \quad (\text{A3a})$$

$$\lim_{n \rightarrow \pm\infty} q_n = 0. \quad (\text{A3b})$$

Recalling the recurrence relation satisfied by Bessel functions⁵⁶

$$2 \frac{dZ_n(\tau)}{d\tau} = Z_{n-1}(\tau) - Z_{n+1}(\tau), \quad (\text{A4})$$

where Z is any Bessel function, and repeating it twice we obtain

$$4 \frac{d^2 Z_n(\tau)}{d\tau^2} = Z_{n+2}(\tau) - 2Z_n(\tau) + Z_{n-2}(\tau). \quad (\text{A5})$$

Comparing (A5) with (A2) we obtain plausible solution for half of the problem. This solution – for even n – is

$$q_n(\tau) = J_{2n}(2\tau), \quad (\text{A6})$$

where J_n is the Bessel function of the first kind.

To obtain a rigorous solution (and for the whole problem) we use Laplace transformation

$$Q_n(s) = \int_0^\infty d\tau e^{-s\tau} q_n(\tau). \quad (\text{A7})$$

For $Q_n(s)$ we obtain the difference equation

$$Q_{n+1}(s) - (2 + s^2)Q_n(s) + Q_{n-1}(s) = -s\delta_{n0}. \quad (\text{A8})$$

Solving (A8) we get

$$Q_n(s) = \frac{1}{\sqrt{s^2 + 4}} \left(\frac{\sqrt{s^2 + 4} - s}{2} \right)^{2|n|}. \quad (\text{A9})$$

Taking into account the inverse Laplace transform correspondence tables⁵⁶, we obtain Eq. (A6) for all n .

2. The quasi-continuum approximation

Now let us calculate the propagator approximately. We'll consider q as a function of the continuous variable z , present Eq. (A2) as

$$\frac{\partial^2 q}{\partial \tau^2} = 2 \sum_{m=1} \frac{1}{(2m)!} \frac{\partial^{2m} q}{\partial z^{2m}}, \quad (\text{A10})$$

and truncate the expansion.

In the continuum approximation Eq. (A2) takes the form

$$\frac{\partial^2 q(z, \tau)}{\partial \tau^2} = \frac{\partial^2 q(z, \tau)}{\partial z^2}. \quad (\text{A11})$$

The propagator is defined by the initial and the boundary conditions

$$q(z, 0) = \delta(z), \quad \frac{\partial q(z, 0)}{\partial \tau} = 0, \quad (\text{A12a})$$

$$\lim_{z \rightarrow \pm\infty} q(z, \tau) = 0. \quad (\text{A12b})$$

The solution is obvious

$$\frac{\partial q(z, \tau)}{\partial \tau} = \frac{1}{2} [\delta(\tau + z) + \delta(\tau - z)]. \quad (\text{A13})$$

The result correctly describes the front motion (see below) but completely misses the structure of the exact solution.

In the quasi-continuum approximation we take into account two terms of the expansion (A10), which modifies Eq. (A11) to

$$\frac{\partial^2 q(z, \tau)}{\partial \tau^2} = \frac{\partial^2 q(z, \tau)}{\partial z^2} + \frac{1}{12} \frac{\partial^4 q(z, \tau)}{\partial z^4}. \quad (\text{A14})$$

Making Laplace transformation with respect to τ and Fourier transformation with respect to z

$$\mathcal{Q}(k, s) = \int_0^\infty d\tau e^{-s\tau} \int_{-\infty}^{+\infty} dz q(z, \tau) e^{ikz}, \quad (\text{A15})$$

we obtain for the propagator equation

$$\left(s^2 + k^2 - \frac{k^4}{12} \right) \mathcal{Q}(k, s) = s. \quad (\text{A16})$$

Solving Eq. (A16) we get

$$\mathcal{Q}(k, s) = \frac{s}{s^2 + k^2 - \frac{k^4}{12}}. \quad (\text{A17})$$

Taking into account the inverse Laplace transform correspondence tables⁵⁶, we obtain

$$q(k, \tau) = \cos \left(\sqrt{k^2 - k^4/12} \tau \right). \quad (\text{A18})$$

In the framework of the approximation we are allowed to consider only $k \ll 1$. Expanding square root with respect to k we obtain

$$q(k, \tau) = \cos \left[(k - k^3/24) \tau \right]. \quad (\text{A19})$$

Presenting cosine function as half sum of two exponents we may write down

$$q(z, \tau) = q^+(z, \tau) + q^+(-z, \tau), \quad (\text{A20})$$

Making inverse Fourier transformation we obtain

$$\begin{aligned} q^+(z, \tau) &= \frac{1}{4\pi} \int_{-\infty}^{+\infty} dk \exp[i(\tau - z)k - i\tau k^3/24] \\ &= \tau^{-1/3} \text{Ai} \left[2\tau^{-1/3}(z - \tau) \right], \end{aligned} \quad (\text{A21})$$

where Ai is the Airy function⁵⁶. After some initial time the $q^+(z, \tau)$ is effectively different from zero only at $z > 0$, and $q^+(-z, \tau)$ – at $z < 0$. Equation (A21) describes the signal front at $z \sim \tau/2$, exponentially small precursor for $\tau < 2z$, and oscillations and power law decrease of the signal in the wake for $\tau > 2z$. The width of the transition region between the two asymptotic forms increases with time as $\tau^{1/3}$.

Fig. 8 compares Eq. (A21) with the exact result (A6) for τ from zero up to a couple of z . To compare the results for $\tau \gg z$, we may use asymptotic forms of Bessel and Airy functions⁵⁶. We have

$$J_{2n}(2\tau) \sim \sqrt{\frac{1}{\pi\tau}} (-1)^n \cos \left(2\tau - \frac{\pi}{4} \right), \quad (\text{A22a})$$

$$\tau^{-1/3} \text{Ai} \left[2\tau^{-1/3}(z - \tau) \right] \sim \sqrt{\frac{1}{\pi\tau}} \cos \left[A\tau \left(1 - \frac{z}{\tau} \right)^{3/2} - \frac{\pi}{4} \right], \quad (\text{A22b})$$

where $A = 2^{5/2}/3 \approx 1.9$.

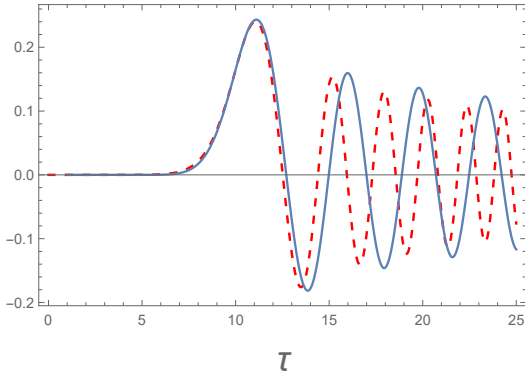


FIG. 8: Propagator calculated for $n = 10$ exactly (Eq. (A6), solid blue line) and for $z = 10$ in the framework of the quasi-continuum approximation (Eq. (A21), dashed red line).

Equations (A19) and (A20) prompt us another approximation for the discrete transmission line – the simple wave approximation¹⁴, which decouples (A14) into two equations for right and left going waves

$$\frac{\partial \varphi}{\partial \tau} \pm \left(\frac{\partial \varphi}{\partial x} + \frac{1}{24} \frac{\partial^3 \varphi}{\partial x^3} \right) = 0. \quad (\text{A23})$$

3. Signalling in the linear transmission line

Consider the discrete semi-infinite linear transmission line, which is characterized by Eq. (A2) for $n \geq 1$ with the initial and the boundary conditions

$$q_n(0) = \dot{q}_n(0) = 0, \quad (\text{A24a})$$

$$q_0(\tau) = \delta(\tau), \quad \lim_{n \rightarrow +\infty} q_n(\tau) = 0. \quad (\text{A24b})$$

For brevity we will call such solution the signal.

The problem can be solved exactly. After Laplace transformation we obtain difference equation

$$Q_{n+1}(s) - (2 + s^2)Q_n(s) + Q_{n-1}(s) = 0 \quad (\text{A25})$$

with the boundary conditions

$$Q_0(s) = 1, \quad \lim_{n \rightarrow +\infty} Q_n(\tau) = 0. \quad (\text{A26})$$

Solving (A25) we get

$$Q_n(s) = \left(\frac{\sqrt{s^2 + 4} - s}{2} \right)^{2n}. \quad (\text{A27})$$

Taking into account the inverse Laplace transform correspondence tables⁵⁶, we obtain^{42,57}

$$q_n(\tau) = \frac{2n}{\tau} J_{2n}(2\tau). \quad (\text{A28})$$

Now let us solve the problem in the framework of the quasi-continuum approximation. We have Eq. (A14), for $z \geq 0$ with the initial and the boundary conditions

$$q(z, 0) = 0, \quad \partial q(z, 0)/\partial \tau = 0, \quad (\text{A29a})$$

$$q(0, \tau) = \delta(\tau), \quad \lim_{z \rightarrow \infty} q(z, \tau) = 0. \quad (\text{A29b})$$

For the Laplace transform we obtain equation

$$\frac{1}{12} \frac{d^4 Q(z, s)}{dz^4} + \frac{d^2 Q(z, s)}{dz^2} = s^2 Q(z, s), \quad (\text{A30})$$

Taking into account the boundary conditions, we can write down the solution of Eq. (A30) as

$$Q(z, s) = e^{k(s)z}. \quad (\text{A31})$$

where k is the negative real root of the polynomial equation

$$\frac{k^4}{12} + k^2 = s^2. \quad (\text{A32})$$

Using Bromwich integral we get

$$q(z, \tau) = \frac{1}{2\pi i} \int_{a-i\infty}^{a+i\infty} ds e^{s\tau + k(s)z}. \quad (\text{A33})$$

In the framework of the quasi-continuum approximation we should expand the solution of (A32) with respect to s to obtain

$$k(s) = -s + s^3/24. \quad (\text{A34})$$

Substituting into (A33) we finally get

$$\begin{aligned} q(z, \tau) &= \frac{1}{2\pi i} \int_{-i\infty}^{+i\infty} ds \exp [s(\tau - z) + zs^3/24] \\ &= 2z^{-1/3} \text{Ai} \left[2z^{-1/3}(z - \tau) \right]. \end{aligned} \quad (\text{A35})$$

Comparing Eqs. (A28) and (A35), and looking at Fig. 9, we realize that in the vicinity of the peak of the signal, the agreement between the exact and the approximate results for the semi-infinite line would be as good, as for the infinite line. However for greater τ the agreement would be worse, because the approximate result decreases with τ slower than the exact one. That is what we see on Fig. 9.

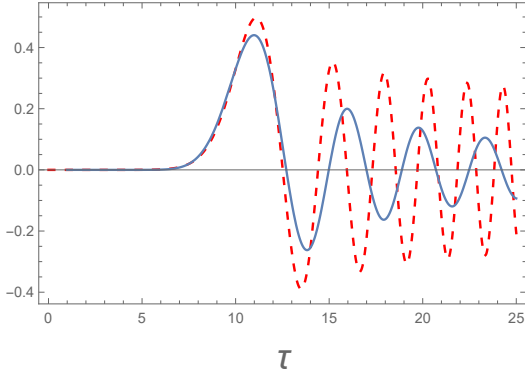


FIG. 9: Signal for the semi-infinite line, calculated for $n = 10$ exactly (Eq. (A28), solid blue line) and for $z = 10$ in the framework of the quasi-continuum approximation (Eq. (A35), dashed red line).

Appendix B: The integral approximation

We must warn the reader that the present Section is mostly of speculative nature. We were not able to advance far on the road we have taken here (if at all). However, some equations obtained in the process look quite amusing to us, and we decided to present them to general attention.

1. The linear transmission line

We consider Eq. (A2) and try to improve the quasi-continuum approximation by expressing the r.h.s. of the equation in the form alternative to the Taylor expansion (A10), thus avoiding the necessity of the truncation of the expansion. Treating q as a function of the continuous variable z (and τ), we approximate Eq. (A2) as

$$\frac{d^2q(z, \tau)}{d\tau^2} = \int_{-\infty}^{+\infty} dz' g(z - z') \frac{d^2q(z', \tau)}{dz'^2}, \quad (\text{B1})$$

where $g(z)$ is a non-singular function, which is positive, even, has zero moment equal to one

$$\int_{-\infty}^{+\infty} dz g(z) = 1, \quad (\text{B2})$$

and goes to zero fast enough when $z \rightarrow \infty$.

Consider again the propagator in the infinite line. Making Laplace transformation with respect to τ and Fourier transformation with respect to z we obtain, starting from (B1), the equation

$$[s^2 + k^2 g(k)] \mathcal{Q}(k, s) = s, \quad (\text{B3})$$

where $g(k)$ is the Fourier image of $g(z)$. The question is whether we can choose some nonsingular function $g(k)$ such, that

$$\frac{1}{2\pi} \int_{-\infty}^{+\infty} dk \cos(k\sqrt{g(k)}\tau) \quad (\text{B4})$$

would emulate the exact solution. Assuming that the answer to this question is "yes, we can", let us try to understand what the approximation similar to (B1) gives for the JTL.

2. The Josephson transmission line

Returning to Eq. (3) and treating φ as a function of the continuous variable z (which we measure in Λ), in line what we have tried previously, let us approximate the equation as

$$\frac{\partial^2 \varphi(z, t)}{\partial \tau^2} = \int_{-\infty}^{+\infty} dz' g(z - z') \frac{d^2 \sin \varphi(z', t)}{dz'^2}. \quad (\text{B5})$$

Looking for the running wave (5) solution of (B5), we obtain the integro-differential equation (the counterpart of (14)) for the function $\varphi(x)$

$$\bar{U}^2 \frac{d^2 \varphi(x)}{dx^2} = \int_{-\infty}^{+\infty} dx' \frac{d^2 g(x - x')}{dx'^2} \sin \varphi(x'). \quad (\text{B6})$$

Integrating Eq. (B6) with respect to x twice we obtain Hammerstein equation of the second kind⁵⁸

$$\bar{U}^2 \varphi(x) = \int_{-\infty}^{+\infty} dx' g(x - x') \sin \varphi(x') - F. \quad (\text{B7})$$

Imposing the boundary conditions (10) and going in Eq. (B7) to the limits $x \rightarrow +\infty$ and $x \rightarrow -\infty$, we recover Eq. (13) and, hence, (??). Substituting \bar{U}^2 and F into Eq. (B7) we get the counterpart of Eq. (7)

$$\begin{aligned} \frac{\sin \varphi_1 - \sin \varphi_2}{\varphi_1 - \varphi_2} \varphi(x) + \frac{\varphi_1 \sin \varphi_2 - \varphi_2 \sin \varphi_1}{\varphi_1 - \varphi_2} \\ = \int_{-\infty}^{+\infty} dx' g(x - x') \sin \varphi(x'). \end{aligned} \quad (\text{B8})$$

Now let us consider Eq. (B8) per se, forgetting the properties of $\varphi(x)$ which were postulated to derive it. We realise that if $\varphi(x)$ goes to some limits when $x \rightarrow +\infty$ and $x \rightarrow -\infty$, each of these limits is either φ_1 , or φ_2 . This is unfortunately all we can say about the equation.

Equation (7) was shown to have the solution only if either $\varphi_2 = \varphi_1$, or $\varphi_2 = -\varphi_1$. We are unable to do the same for Eq. (B8), which raises the question whether the relations between the asymptotic phases on both sides of the running wave, obtained in Sections III and IV, are the exact ones, or only approximate. This remains unclear for us.

However, the relation $\varphi_2 = \varphi_1$ being imposed, Eq. (B8) takes the form

$$\frac{\sin \varphi_1}{\varphi_1} \varphi(x) = \int_{-\infty}^{+\infty} dx' g(x - x') \sin \varphi(x') . \quad (\text{B9})$$

This equation is the counterpart of Eq. (7). The only thing we can prove about the solution of Eq. (B9) is

that, for any x ,

$$-\varphi_1 \leq \varphi(x) \leq \varphi_1 \quad (\text{B10})$$

(for the sake of definiteness we consider φ_1 to be positive). In fact, let $\sin \varphi(x)$ reaches maximum value at some point x_0 , and $\sin \varphi(x_0) > \sin \varphi_1$. Then on one hand

$$\int_{-\infty}^{+\infty} dx' g(x - x') \sin \varphi(x') < \sin \varphi(x_0) , \quad (\text{B11})$$

on the other hand

$$\frac{\sin \varphi_1}{\varphi_1} \varphi(x_0) > \sin \varphi(x_0) , \quad (\text{B12})$$

because $\sin \varphi/\varphi$ decreases when $\sin \varphi$ increases for positive φ . So we came to a contradiction. Similar for the minimum value of $\sin \varphi$.

^{*} Electronic address: Eugene.Kogan@biu.ac.il

¹ G. B. Whitham, *Linear and Nonlinear Waves*, John Wiley & Sons Inc., New York (1999).

² D. M. French and B. W. Hoff, IEEE Trans. Plasma Sci. **42**, 3387 (2014).

³ B. Nouri, M. S. Nakhla, and R. Achar, IEEE Trans. Microw. Theory Techn. **65**, 673 (2017).

⁴ L. P. S. Neto, J. O. Rossi, J. J. Barroso, and E. Schamiloglu, IEEE Trans. Plasma Sci. **46**, 3648 (2018).

⁵ M. S. Nikoo, S. M.-A. Hashemi, and F. Farzaneh, IEEE Trans. Microw. Theory Techn. **66**, 3234 (2018); **66**, 4757 (2018).

⁶ L. C. Silva, J. O. Rossi, E. G. L. Rangel, L. R. Raimundi, and E. Schamiloglu, Int. J. Adv. Eng. Res. Sci. **5**, 121 (2018).

⁷ Y. Wang, L.-J. Lang, C. H. Lee, B. Zhang, and Y. D. Chong, Nat. Comm. **10**, 1102 (2019).

⁸ E. G. L. Range, J. O. Rossi, J. J. Barroso, F. S. Yamasaki, and E. Schamiloglu, IEEE Trans. Plasma Sci. **47**, 1000 (2019).

⁹ A. S. Kyuregyan, Semiconductors **53**, 511 (2019).

¹⁰ N. A. Akem, A. M. Dikande, and B. Z. Essimbi, SN Applied Science **2**, 21 (2020).

¹¹ A. J. Fairbanks, A. M. Darr, A. L. Garner, IEEE Access **8**, 148606 (2020).

¹² R. Landauer, IBM J. Res. Develop. **4**, 391 (1960).

¹³ S. T. Peng and R. Landauer, IBM J. Res. Develop. **17**(1973).

¹⁴ M. I. Rabinovich and D. I. Trubetskoy, *Oscillations and Waves*, Kluwer Academic Publishers, Dordrecht / Boston / London (1989).

¹⁵ B. D. Josephson, Phys. Rev. Lett. **1**, 251 (1962).

¹⁶ A. Barone and G. Paterno, *Physics and Applications of the Josephson Effect*, John Wiley & Sons, Inc, New York (1982).

¹⁷ N. F. Pedersen, Solitons in Josephson Transmission lines, in *Solitons*, North-Holland Physics Publishing, Amsterdam (1986).

¹⁸ C. Giovanella and M. Tinkham, *Macroscopic Quantum Phenomena and Coherence in Superconducting Networks*, World Scientific, Frascati (1995).

¹⁹ A. M. Kadin, *Introduction to Superconducting Circuits*, Wiley and Sons, New York (1999).

²⁰ M. Remoissenet, *Waves Called Solitons: Concepts and Experiments*, Springer-Verlag Berlin Heidelberg GmbH (1996).

²¹ O. Yaakobi, L. Friedland, C. Macklin, and I. Siddiqi, Phys. Rev. B **87**, 144301 (2013).

²² K. O'Brien, C. Macklin, I. Siddiqi, and X. Zhang, Phys. Rev. Lett. **113**, 157001 (2014).

²³ C. Macklin, K. O'Brien, D. Hover, M. E. Schwartz, V. Bolkhovsky, X. Zhang, W. D. Oliver, and I. Siddiqi, Science **350**, 307 (2015).

²⁴ B. A. Kochetov, and A. Fedorov, Phys. Rev. B. **92**, 224304 (2015).

²⁵ A. B. Zorin, Phys. Rev. Applied **6**, 034006 (2016); Phys. Rev. Applied **12**, 044051 (2019).

²⁶ D. M. Basko, F. Pfeiffer, P. Adamus, M. Holzmann, and F. W. J. Hekking, Phys. Rev. B **101**, 024518 (2020).

²⁷ T. Dixon, J. W. Dunstan, G. B. Long, J. M. Williams, Ph. J. Meeson, C. D. Shelly, Phys. Rev. Applied **14**, 034058 (2020).

²⁸ A. Burshtein, R. Kuzmin, V. E. Manucharyan, and M. Goldstein, Phys. Rev. Lett. **126**, 137701 (2021).

²⁹ T. C. White et al., Appl. Phys. Lett. **106**, 242601 (2015).

³⁰ A. Miano and O. A. Mukhanov, IEEE Trans. Appl. Supercond. **29**, 1501706 (2019).

³¹ Ch. Liu, Tzu-Chiao Chien, M. Hatridge, D. Pekker, Phys. Rev. A **101**, 042323 (2020).

³² P. Rosenau, Phys. Lett. A **118**, 222 (1986); Phys. Scripta **34**, 827 (1986).

³³ A. Houwe, S. Abbagari, M. Inc, G. Betchewe, S. Y. Doka, K. T. Crepin, and K. S. Nisar, Results in Physics **18**, 103188 (2020).

³⁴ D. L. Sekulic, N. M. Samardzic, Z. Mihajlovic, and M. V. Sataric, Electronics **10**, 2278 (2021).

³⁵ P. G. Kevrekidis, I. G. Kevrekidis, A. R. Bishop, and E. Titi, Phys. Rev. E, **65**, 046613 (2002).

³⁶ L. Q. English, F. Palmero, A. J. Sievers, P. G. Kevrekidis, and D. H. Barnak, Phys. Rev. E, **81**, 046605 (2010).

³⁷ P. G. Kevrekidis, IMA Journal of Applied Mathematics **76**, 389 (2011)

³⁸ V. Nesterenko, *Dynamics of heterogeneous materials*, Springer Science & Business Media (2013).

³⁹ B. A. Malomed, *The sine-gordon model: General background, physical motivations, inverse scattering, and solitons*, The Sine-Gordon Model and Its Applications. Springer, Cham, 1-30 (2014).

⁴⁰ V. F. Nesterenko, Phil. Trans. R. Soc. A **376**, 20170130 (2018).

⁴¹ B. A. Malomed, *Nonlinearity and discreteness: Solitons in lattices*, Emerging Frontiers in Nonlinear Science. Springer, Cham, 81 (2020).

⁴² E. Kogan, Journal of Applied Physics **130**, 013903 (2021).

⁴³ H. R. Mohebbi and A. H. Majedi, IEEE Trans. Appl. Supercond. **19**, 891 (2009); IEEE Transactions on Microwave Theory and Techniques **57**, 1865 (2009).

⁴⁴ G. J. Chen and M. R. Beasley, IEEE Trans. Appl. Supercond. **1**, 140 (1991).

⁴⁵ H. Katayama, N. Hatakenaka, and T. Fujii, Phys. Rev. D **102**, 086018 (2020).

⁴⁶ S. Homma, Prog. Theor. Phys. **76**, 1(1986).

⁴⁷ E. B. Herbold and V. F. Nesterenko, Phys. Rev E, **75**, 021304, (2007).

⁴⁸ T. H. A. van der Reep, Phys. Rev. A **99**, 063838 (2019).

⁴⁹ L Fasolo, A Greco, E Enrico, in *Advances in Condensed-Matter and Materials Physics: Rudimentary Research to Topical Technology*, (ed. J. Thirumalan and S. I. Pokutny), Scence (2019).

⁵⁰ A. Greco, L. Fasolo, A. Meda, L. Callegaro, and E. Enrico, Phys. Rev. B 104, 184517 (2021).

⁵¹ Y. Yuan, M. Haider, J. A. Russer, P. Russer and C. Jirauschek, 2020 XXXIIrd General Assembly and Scientific Symposium of the International Union of Radio Science, Rome, Italy (2020).

⁵² Z. K. Minev, Th. G. McConkey, M. Takita, A. D. Corcoles, and J. M. Gambetta, arXiv:2103.10344 (2021).

⁵³ E. Bettelheim and L. I. Glazman, Phys. Rev. Lett. **109**, 260602 (2012).

⁵⁴ Th. Veness and L. I. Glazman, Phys. Rev. B **100**, 235125 (2019).

⁵⁵ A. Mandilara, C. Valagiannopoulos, and V. M. Akulin, Phys. Rev. A **99**, 023849 (2019).

⁵⁶ M. Abramowitz, I. A. Stegun eds., *Handbook of Mathematical Functions with Formulas, Graphs, and Mathematical Tables*, (National Bureau of Standards, Washington, 1964).

⁵⁷ N. Kwidzinski and R. Bulla, arXive1608.0061.

⁵⁸ F. G. Tricomi, *Integral equations*, (Mineola, NY: Dover-Publications, 1982).